Quantification of site disorder and its role on spin polarization in the nearly half-metallic Heusler alloy NiFeMnSn

M. D. Mukadam, Syamashree Roy, S. S. Meena, Pramod Bhatt, and S. M. Yusuf*
Solid State Physics Division, Bhabha Atomic Research Centre, Mumbai 400085, India
(Received 29 June 2016; revised manuscript received 21 October 2016; published 21 December 2016)

The electronic structure and magnetism of the quaternary Heusler alloy NiFeMnSn are studied using the full-potential linearized augmented plane-wave (FPLAPW) method. The calculation for the perfectly LiMgPdSn-type ordered crystal structure (type I) of NiFeMnSn shows a high spin polarization (∼76%) with a ferromagnetic ground state. The total spin magnetic moment is in good agreement with the Slater-Pauling rule. The structural investigations using neutron diffraction at 500 K, and Mössbauer spectroscopy at 300 K on the NiFeMnSn alloy, prepared using an arc melting, show the presence of atomic site disorder. The electronic structure calculation for the disordered structure shows that the site disorder destroys the nearly half-metallic nature of this alloy. The magnetization measurements indicate that the Curie temperature is well above room temperature (∼405 K) as desired for the spintronics application.

DOI: 10.1103/PhysRevB.94.214423

I. INTRODUCTION

Spin-polarized ferromagnetic materials with high Curie temperatures are important in the area of magnetoelectronics or spintronics [1]. Half-metallic materials, which are metallic for one spin direction, and semiconducting for the other spin direction, exhibit a complete spin polarization at the Fermi level as predicted for half-Heusler alloys by de Groot *et al.* [2,3] in the early 1980s. High spin polarization in such materials can play a significant role in new generation devices where standard microelectronic devices are combined with spin-dependent effects [4,5]. A typical application of such materials is a magnetic random access memory (MRAM), which utilizes the magnetoresistance. Heusler alloys with the $L2_1$ structure are of more interest in this regard as some of these alloys exhibit high Curie temperatures with large magnetic moment per unit cell; and according to theory, such alloys should exhibit a high spin polarization [6,7].

In view of this, ternary intermetallic Heusler compounds X_2YZ with $L2_1$ structure (four fcc sublattices occupied by three atoms X, Y, and Z), where X and Y are transition or rare-earth metals, and Z is a main-group element, have been studied extensively. Besides half-metallic ferromagnetism [6], a large variety of other properties, such as magnetic shape memory [8], giant magnetocaloric effect [9], thermoelectrics [10], and superconductivity [11] are reported in such materials. Moreover, the ternary intermetallic compounds are doped to form pseudoternary systems in order to tune their various properties including the tuning of the Fermi energy to the middle of the gap in one spin channel [12,13]. It is shown in the literature that pseudoternary Heusler alloys with composition $X_2Y_{1-a}Y'_aZ$ with a random distribution of Y and Y' have disadvantage due to an additional disorder electron scattering and the resulting short spin diffusion length [14,15]. However, the quaternary 1:1:1:1 Heusler systems [16,17], termed as equiatomic quaternary Heusler alloys, where each of the four interpenetrating fcc lattices of the $L2_1$ Heusler structure (space group $Fm\bar{3}m$) is occupied by different atoms forming a LiMgPdSn type, called the Y-type structure with space group $F\bar{4}3m$, have an advantage due to the absence of such a disorder scattering [14]. Such quaternary Heusler alloys are relatively less explored. Bainsla *et al.* have revealed that the electronic structure and hence the physical properties strongly depend on the atomic site disorder in the quaternary Heusler alloy system [14], making it quite essential to understand the atomic site disorder and its role on electronic structure.

In the present article, we report the results of an electronic structure calculation along with experimental results of structural and magnetic properties of the equiatomic quaternary Heusler alloy, NiFeMnSn. We have quantified the atomic site disorder from neutron diffraction and Mössbauer spectroscopy investigations, and revealed from the electronic structure calculation that the derived atomic site disorder destroys the high spin polarization in this intermetallic Heusler alloy. The present results on the quantitative determination of structural disorder and its role in modifying the spin polarization are important in the area of spintronics involving Heusler alloys.

II. EXPERIMENTAL AND THEORETICAL METHODOLOGIES

NiFeMnSn ingots were prepared by an arc melting of the appropriate amounts of the constituent elements in an argon atmosphere under an ambient pressure condition. The purity of the starting constituents was 99.9% mass fraction or better. The ingots were flipped and remelted several times to ensure a good homogeneity. After melting, the ingots were wrapped in a Ta foil, and annealed at 800 °C for a week in an evacuated quartz tube for better homogenization.

The crystal structure of the prepared sample was analyzed by x-ray diffraction (XRD) using a Cu Kα radiation. Dc magnetization (M) measurements were carried out as a function of temperature (T) and magnetic field (H) using a vibrating sample magnetometer (Cryogenic Ltd., UK make). To understand the local environment of Fe, Mössbauer spectrum for NiFeMnSn alloy was recorded at room temperature using a constant acceleration spectrometer with a ^{57}Co(Rh) radioactive source.

*smyusuf@barc.gov.in

Unpolarized neutron diffraction data were recorded at 5, 300, and 500 K using the five linear position sensitive detector based powder diffractometer II at the Dhruva Reactor, Mumbai, India. For neutron diffraction measurements, the powdered sample was placed in a vanadium can, and data were collected over the scattering angular (2θ) range of 4.5° to 138° in steps of 0.05° with a wavelength of 1.2443 Å.

The electronic structure calculations (at $T = 0$ K) were performed by means of the full-potential linearized augmented plane-wave (FLAPW) method as implemented in WIEN2K [18]. The exchange correlation functional was taken within the generalized gradient (GGA) approximation in the parametrization of Perdew *et al.* [19]. The number of plane waves was restricted by $R_{\mathrm{MT}}k_{\mathrm{max}} = 9$. All self-consistent calculations were performed with 455 k points in the irreducible wedge of the Brillouin zone, based on a $25 \times 25 \times 25$ point mesh. The energy convergence criterion was set to 10^{-5} Ry, and simultaneously the charge convergence was set to $10^{-3}e$.

III. RESULTS AND DISCUSSION

Figure 1 shows the observed and the Rietveld refined XRD patterns at room temperature for the NiFeMnSn Heusler alloy. The observed XRD pattern reveals a highly crystalline nature of the sample. Rietveld refinement of the XRD pattern was performed with the FULLPROF program in the WINPLOTR suite of programs [20]. The analysis confirms the LiMgPdSn-type Heusler structure with the space group $F\bar{4}3m$ with a lattice parameter of 6.030(1) Å. The LiMgPdSn-type Heusler structure consists of four interpenetrating fcc lattices, occupied by different atoms (space group $F\bar{4}3m$) as shown in Fig. 2. Three nonequivalent fully ordered crystal structures (under the LiMgPdSn type), namely types I, II, and III are possible. For the type-I structure, the Wyckoff positions 4*a* (0, 0, 0), 4*b* ($\frac{1}{2}$, $\frac{1}{2}$, $\frac{1}{2}$), 4*c* ($\frac{1}{4}$, $\frac{1}{4}$, $\frac{1}{4}$), and 4*d* ($\frac{3}{4}$, $\frac{3}{4}$, $\frac{3}{4}$) are occupied by Sn, Mn, Fe, and Ni atoms, respectively. The type-II (III) structure is

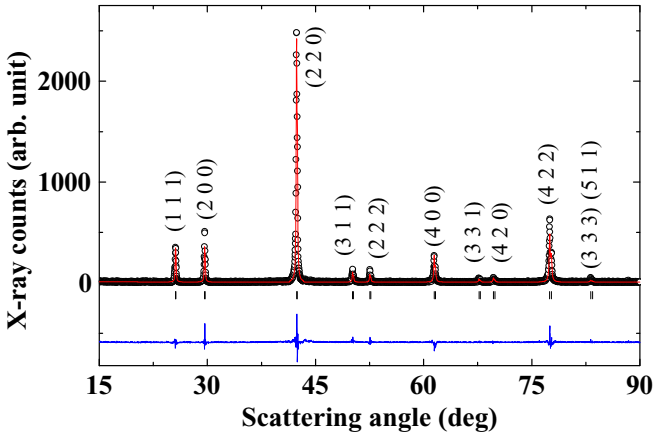

FIG. 1. Observed room-temperature x-ray diffraction pattern of NiFeMnSn Heusler alloy is shown by open circles. Rietveld refined pattern is shown by solid line. Solid line at the bottom shows the difference between the observed and calculated patterns. The vertical bars indicate the position of allowed Bragg peaks. The (*hkl*) values corresponding to the Bragg peaks are also shown.

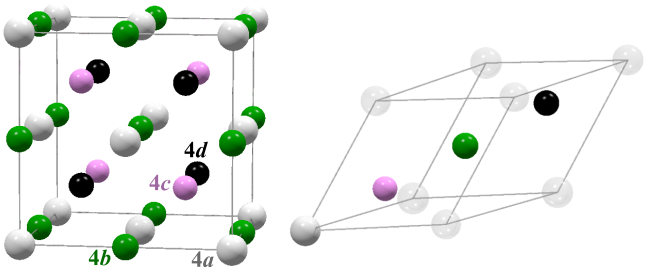

FIG. 2. Crystal structure of the quaternary Heusler compound NiFeMnSn. There are three nonequivalent structures for NiFeMnSn, depending on the occupation at the four different lattice sites 4*a* (light gray with larger radius), 4*b* (dark gray), 4*c* (medium gray), and 4*d* (black).

realized by placing Sn, Fe, Mn, Ni (Fe, Mn, Sn, Ni) at 4*a*, 4*b*, 4*c*, and 4*d* sites, respectively. Since the x-ray scattering amplitudes of all the constituent elements are very close, it is almost impossible to distinguish between types I, II, and III for this compound from the analysis of the XRD pattern. We have, therefore, used Mössbauer spectroscopy and neutron diffraction techniques to determine the atomic site distribution (disorder) in the studied Heusler alloy.

In order to understand the various possible environments and the site occupancies of the Fe atom, the ^{57}Fe Mössbauer spectroscopy was carried out at room temperature. Figure 3 depicts the Mössbauer spectrum for the NiFeMnSn alloy, recorded at 300 K, showing the presence of three sextets and a singlet. For a fully ordered type-I crystal structure, Fe atoms occupy the 4*c* site only. With respect to the Fe atoms, the first nearest neighbor (1NN) sites are occupied by four Mn and four Sn atoms, while the second nearest neighbor (2NN) sites are occupied by six Ni atoms. Hence, a single sextet alone is expected. But the presence of three sextets (contributing ~52, 15, and 24% to the total integrated intensity) and a singlet (relative intensity ~9%) suggests an occurrence of a structural (site) disorder with regard to Fe atoms. The values of the hyperfine magnetic field (H_{hf}), quadrupole splitting (Δ), isomer shift (δ), and relative areas (RA) for Fe sites in

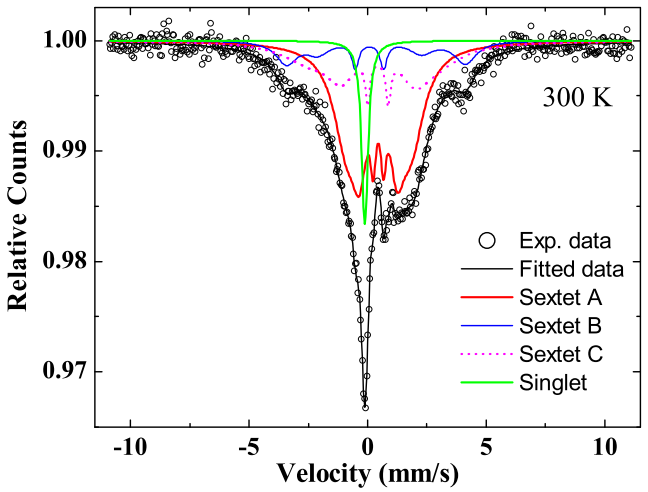

FIG. 3. The Mössbauer spectrum for NiFeMnSn Hesuler alloy at 300 K.

TABLE I. The hyperfine magnetic field (H_{hf}), quadrupole splitting (Δ), isomer shift (δ), and relative areas (RA) for Fe sites in NiFeMnSn alloy derived from the Mössbauer spectrum recorded at 300 K. Isomer shift values are relative to Fe metal foil ($\delta = 0.0$ mm/s).

Fe Sites	H_{hf} (T)	Δ (mm/s)	δ (mm/s)	RA (%)
Sextet A	8.4 ± 3	0.02 ± 0.02	0.46 ± 0.03	52
Sextet B	23.4 ± 3	0.27 ± 0.03	0.21 ± 0.03	15
Sextet C	16.9 ± 3	−0.23 ± 0.02	0.32 ± 0.03	24
Singlet			−0.11 ± 0.03	9

NiFeMnSn alloy derived from the Mössbauer spectrum have been listed in Table I. The three sextets have average hyperfine fields H_{hf} of 8.4, 23.4, and 16.9 T with quadrupole splitting of 0.02, 0.27, and −0.23 mm/s, respectively. Such types of structural disorder have been reported for other quaternary Heusler alloys in the literature. For example, Bainsla *et al.* [21] reported two sextets with H_{hf} of 28.5 T (corresponding to the $L2_1$ structure) and 10.4 T (corresponding to the DO_3 disordered structure) with relative intensities of 67% and 33%, respectively, from the Mössbauer spectroscopy study of their quaternary Heusler alloy sample CoFeMnGe. From the experimental study on another quaternary Heusler alloy CoFeMnSi, Bainsla *et al.* [22] reported three sextets (with H_{hf} values of 29.0, 13.2, and 9.8 T) and a doublet with the relative intensities of 38%, 35%, 17%, and 10%, respectively, instead of a single sextet, indicating the structural disorder in their alloy sample.

To get more insight into the structural disorder in this NiFeMnSn alloy, we carried out a neutron diffraction experiment at 5, 300, and 500 K. Neutron diffraction is more sensitive to site disorder than x-ray diffraction because of its ability to distinguish adjacent atoms in the periodic table whose neutron coherent scattering amplitudes are vastly different [23,24]. Besides that, the neutron diffraction study reveals the microscopic nature of magnetic ordering of the present system. Figure 4 depicts the Rietveld refined (using the FULLPROF program in the WINPLOTR suite of programs [20]) neutron diffraction patterns at 5, 300, and 500 K. In order to find out the atomic site disorder, the Rietveld refinement was performed for the neutron diffraction pattern recorded in the paramagnetic state at $T = 500$ K (as evident from our dc magnetization data presented later in Fig. 5). The lattice constant of $a = 6.0567(1)$ Å is derived from the refinement (space group $F\bar{4}3m$). We observe that besides the type-I crystal structure, the disorder in the occupancies results into type-II and type-III structures as well in this sample (Table II). Considering these occupancies, it turns out that types I, II, and III with ∼63.3, 13.4, and 23.3%, respectively, are present. This implies that the 4*a*, 4*b*, 4*c*, and 4*d* sites have atomic site disorder of 23.3, 13.4, 36.7, and 0%, respectively, with respect to the type-I structure. Following the Rietveld refinement of the high temperature (500 K) neutron diffraction data, the patterns at 300 and 5 K are refined to reveal the microscopic nature of magnetic ordering of the present system at these temperatures. The derived values of the lattice constant are 6.0470(2) and 6.0245(2) Å at 300 and 5 K, respectively. The site-averaged

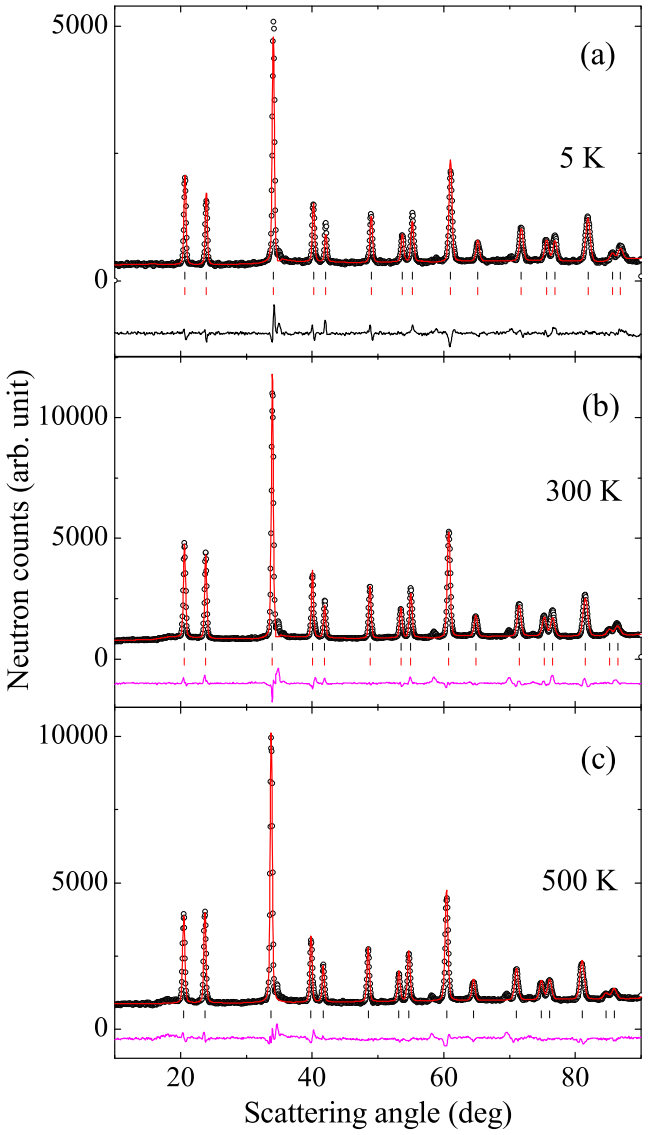

FIG. 4. Observed neutron diffraction patterns of NiFeMnSn Heusler alloy at (a) 5, (b) 300, and (c) 500 K are shown by open circles. Rietveld refined patterns [(a) and (b) nuclear and magnetic; (c) only nuclear] are shown by solid lines. Solid lines at the bottom show the difference between the observed and calculated patterns. The vertical bars indicate the position of allowed Bragg peaks.

moments derived from the refinement at 300 and 5 K are listed in Table II. The total magnetic moments are found to be 2.9 and 4.2 μ_B per formula unit at 300 and 5 K, respectively. Based on the findings from the neutron diffraction study, we can explain the observed three sextets in the Mössbauer spectrum (Fig. 3). The sextet which contributes ∼52% of the total relative intensity ($H_{hf} = 8.4$ T) in the Mössbauer spectrum, can be attributed to the Fe atoms occupying the 4*c* site, which is the case for the type-I ordered crystal structure. The second sextet with a relative intensity of 15% ($H_{hf} = 23.4$ T) could be attributed to Fe atoms occupying the 4*b* site as per the type-II structure, and the third sextet with a relative intensity of 24% ($H_{hf} = 16.9$ T) could be a result of Fe occupying the 4*a* site, corresponding to the type-III structure. The

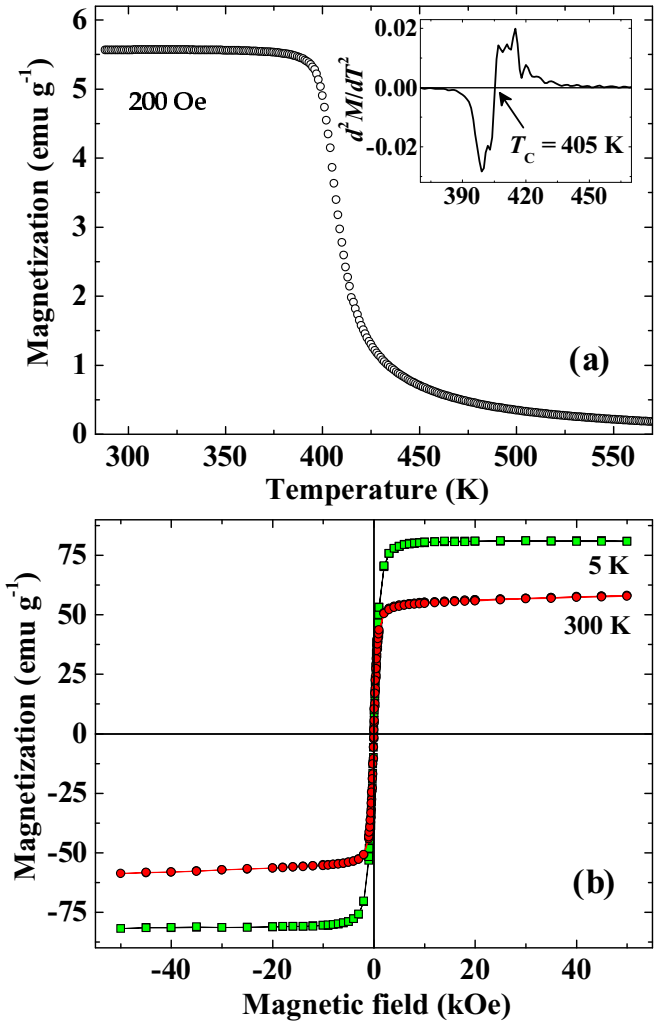

FIG. 5. (a) Temperature dependence of magnetization under the 200-Oe field for NiFeMnSn Heusler alloy. Inset shows the d^2M/dT^2 vs T showing the Curie temperature T_C. (b) Magnetization as a function of the applied magnetic field at 5 and 300 K.

TABLE II. Site occupancies in NiFeMnSn alloy derived from the neutron diffraction pattern at 500 K, and site-averaged ordered magnetic moments (μ_{ord}) as derived from the neutron diffraction patterns at 300 and 5 K. Occupancies were varied freely for the refinement of the neutron diffraction pattern at 500 K. The values in the last column are the occupancies considered for calculating the DOS (Fig. 7) for the structure with atomic site disorder. The values in brackets indicate an error in last digit of μ_{ord}.

Site (x,y,z)	Atom	Occupancy	$\mu_{ord}(\mu_B)$ 300 K	$\mu_{ord}(\mu_B)$ 5 K	Occupancy for DOS
4a (0, 0, 0)	Sn	0.767(1)	0.2(1)	0.3(1)	0.75
	Fe	0.233(1)			0.25
4b ($\frac{1}{2}$, $\frac{1}{2}$, $\frac{1}{2}$)	Mn	0.866(1)	1.8(2)	2.5(2)	0.875
	Fe	0.134(1)			0.125
4c ($\frac{1}{4}$, $\frac{1}{4}$, $\frac{1}{4}$)	Fe	0.633(1)	0.7(1)	0.9(1)	0.625
	Mn	0.134(1)			0.125
	Sn	0.233(1)			0.25
4d ($\frac{3}{4}$, $\frac{3}{4}$, $\frac{3}{4}$)	Ni	1.000(1)	0.2(1)	0.3(1)	1.0

presence of further structural disorder, causing a paramagnetic-like state, has been confirmed from the observed singlet in the Mössbauer spectrum with a relative intensity of ∼9%. We will discuss further about the hyperfine magnetic fields later.

The magnetic properties are also studied by measuring dc magnetization as a function of temperature and magnetic field. Figure 5(a) shows the magnetization as a function of temperature under the 200-Oe field. A paramagnetic to ferromagnetic transition is quite evident from the M vs T curve. The Curie temperature ($T_C = 405$ K) is derived from the second derivative of the M vs T curve as depicted in the inset of Fig. 5(a). The field-dependent magnetization curves at 5 and 300 K are shown in Fig. 5(b). The observed value of saturation magnetization $M_S \sim 81.0$ emu g^{-1} at 5 K corresponds to 4.18 μ_B per formula unit, which is very close to that observed (4.2 μ_B per formula unit) from the neutron diffraction study at 5 K. At 300 K, M_S is found to be ∼57.8 emu g^{-1} (3.0 μ_B per formula unit), comparable to that observed from the neutron diffraction study (∼2.9 μ_B per formula unit).

Now we present the results of our electronic structure calculation to bring out the implications of site disorder on the spin polarization. We have performed the energy minimization as a function of lattice constant to obtain the true structural ground state of the present Heusler alloy. All three nonequivalent structures under the LiMgPdSn-type viz. types I, II, and III (Fig. 2), are considered for optimizing the lattice parameters, and finding the minimum total energy as a function of the lattice parameter. Figure 6 shows the differences of total energies ($E - E_0$) as a function of lattice constant for all three nonequivalent structures considering two cases: the nonmagnetic (NM) state and the ferromagnetic (FM) state. Spin-polarized electronic structure calculation was done for realization of the ferromagnetic state. Here, E_0 is the minimum energy after considering all three types and both magnetic states. As evident from Fig. 6, the type-I structure with an FM ground state has the lowest total energy indicating that the type-I structure with FM configuration is the preferred structure.

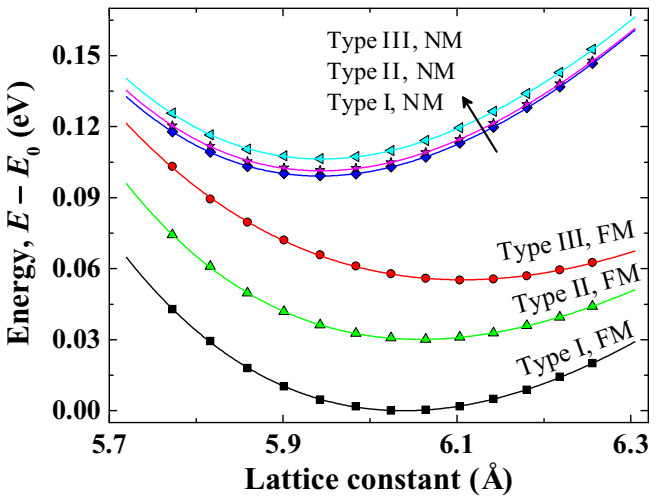

FIG. 6. Energy ($E - E_0$) versus lattice parameter of three possible different crystal structures for both NM and FM spin configurations.

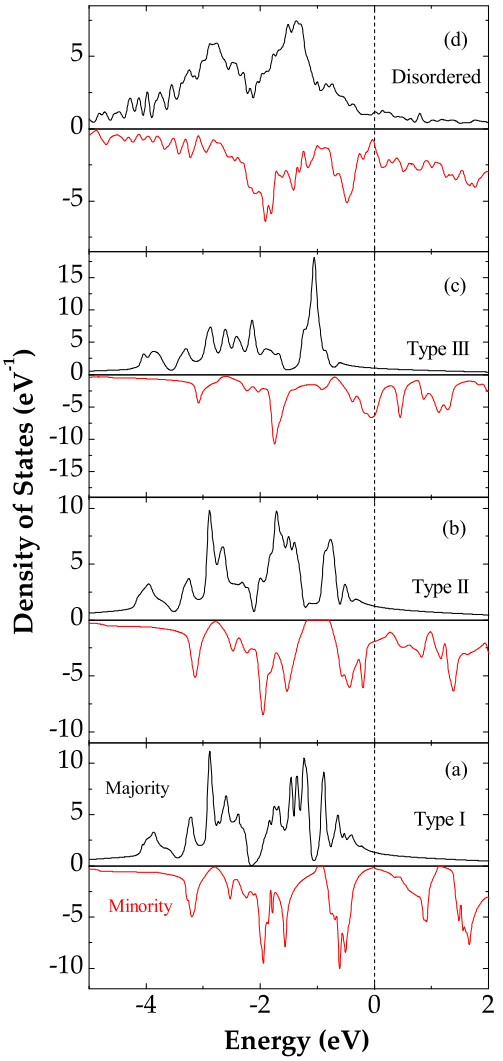

FIG. 7. Spin-polarized densities of states plots for the NiFeMnSn Heusler alloy for (a) type-I, (b) type-II, and (c) type-III structures. (d) DOS plots for the structure with atomic site disorder as shown in Table II.

The optimized lattice parameter (for the type-I structure) is found to be 6.038 Å. It may be noted here that this optimized lattice parameter is in good agreement with that obtained from the neutron diffraction study [$a = 6.0245(2)$ Å] at 5 K. The total energy of the FM type-I structure is lower by 30.15 and 55.30 meV than that for the FM type-II and type-III structures, respectively. However, the neutron diffraction and Mössbauer studies reveal the presence of all three types of structures for the studied alloy. Hence, besides the type-I structure, we also calculated total density of states (DOS) for type-II and type-III structures (Fig. 7). The calculated lattice constants for type-II and type-III structures are found to be 6.057 and 6.106 Å, respectively (Fig. 6). The magnetic moments of all atoms for type-I, -II, and -III crystal structures are listed in Table III. For the type-I structure, which forms the major component of the sample, the total DOS at the Fermi energy (E_F) for majority and minority spins are calculated to be $\rho_\uparrow(E_F) = 1.323$, and $\rho_\downarrow(E_F) = 0.177$ states/eV, respectively. The spin polarization

TABLE III. The atomic magnetic moments and the total magnetic moment (M_{tot}) at $T = 0$ K obtained from the electronic structure calculation.

	Magnetic moments (μ_B)		
Atom	Type I	Type II	Type III
Sn	−0.04	−0.03	−0.08
Mn	3.24	2.41	3.22
Ni	0.45	0.34	0.41
Fe	1.42	2.54	2.32
M_{tot} (μ_B/f.u.)	5.01	5.21	5.78

P is estimated by the following expression:

$$P = \frac{\rho_\uparrow(E_F) - \rho_\downarrow(E_F)}{\rho_\uparrow(E_F) + \rho_\downarrow(E_F)}. \quad (1)$$

The spin polarization is calculated to be ∼76%. The calculated atom resolved spin magnetic moment values are 0.45, 3.24, 1.42, and $-0.04\,\mu_B$ for Ni, Mn, Fe, and Sn, respectively. The very small moment found at the Sn site is mainly due to the polarization of this atom by the surrounding magnetically active atoms. The large total spin magnetic moment (for the type-I structure) of $\sim 5\,\mu_B$ is in good agreement with the Slater-Pauling (SP) rule for an ordered compound with four different kinds of atoms, where $M_{Total} = NV - 24$ [25]. Here NV is the accumulated number of valence electrons in the unit cell. The electronic structure calculations for the type-II and type-III structures show [as evident in Figs. 7(b) and 7(c)] a destruction of the spin polarization for these two types of structures. The total magnetic moment per formula unit increases with changing structures from type I to type II to type III. Noninteger values of total spin magnetic moment (5.21 and 5.78 μ_B per formula unit for type-II and type-III structures, respectively) suggest that the moments for the type-II and type-III structures do not follow the Slater-Pauling (SP) rule [25], usually followed by the half-metallic Heusler alloy systems.

It is evident from the results of the neutron diffraction and Mössbauer studies that all three types (I, II, and III) of structures coexist in the present sample. However, there could be a possible alternate interpretation of the occupancies listed in Table II (derived from the neutron diffraction) by considering a homogeneously disordered crystal structure. In view of this, we have carried out further electronic structure calculation by constructing a supercell consisting of a total 32 atoms to take into account the atomic site disorder. For this purpose, the atoms at four sites (4a,4b,4c, and 4d) are swapped in such a way that the atomic site disorder is as close as possible to that obtained from the neutron diffraction study (Table II) while restricting to a 32-atom supercell. The DOS for the structure with the atomic site disorder [shown in Fig. 7(d)] indicate that the disordered structure does not show any half-metallicity. In other words, the disorder destroys the half-metallic nature. Though the experimental values of total magnetic moments obtained from the dc magnetization

(4.18 μ_B per formula unit) and neutron diffraction (4.2 μ_B per formula unit) at 5 K for the studied system are close, they differ significantly from the calculated ground-state value of 5.96 μ_B (per formula unit) for the structure with the site disorder. This observation of reduced experimental values of magnetic moments is very similar to that found by Svyazhin *et al.* [26] for the Co_2CrAl Heusler alloy. Shinohara *et al.* [27] reported that the reduction in magnetization for the ferromagnetic Heusler alloy sample Pd_2MnSn was due to the severely stressed state rather than to the atomic site disorder.

Now we compare the hyperfine magnetic fields (Table I) obtained from the Mössbauer study with that derived from the present electronic structure calculations, and conclude that the disordered structure, considering a supercell of 32 atoms [Fig. 7(d)], does not represent the system under consideration. Our calculation shows that for the disordered structure there are eight inequivalent Fe sites having H_{HF} over 18.0–26.7 T. It is therefore evident that these calculated H_{HF} values are not consistent with the observed H_{HF} values (8.4, 23.4, and 16.9 T) from the Mössbauer study (shown in Table I). On the other hand, the hyperfine field values obtained from the Mössbauer study follow a trend which is consistent with that (10.3, 30.0, and 19.9 T) derived from the electronic structure calculations for the type-I, -II, and -III structures, respectively. This helps us to confirm that the present NiFeMnSn Heusler alloy is made up of three distinct types (I, II, and III) of crystal structures rather than the "homogeneously" disordered structure. The reduction in the observed hyperfine magnetic fields at 300 K compared to the calculated values (at $T = 0$ K) could be due the thermal effect and also due to the presence of atomic disorder as reflected in both neutron diffraction and Mössbauer spectroscopy studies.

The present calculations show a high spin polarization (∼76%) only for the type-I ordered crystal structure; while the type II and type III as well as the "homogeneously" disordered structures destroy the spin polarization. It is, therefore, essential to avoid the structural disorder ("homogeneous" disorder as well as any mixed state of the types I, II, and/or III) in the Heusler alloy to achieve a high spin polarization. Though the majority of theoretical calculations assume a perfect structural ordering, in practice an alloy processing leads to a site disorder, resulting in a reduction in spin polarization as evident from the present electronic structure calculation. In Co_2FeSi, an $A2$-type site disorder (where Fe and Si atoms occupy their sites at random) resulted in a reduction in spin polarization [28]. Difference in spin polarization between thin films of Co_2FeAl with $L2_1$- and $B2$-type (for $B2$-type structures, Co-Fe and Co-Al disorders take place) structures was reported by Miura *et al.* [29]. In the case of NiCoMnAl, the disordered $B2$ structure was reported to destroy the half-metallicity expected from the perfectly ordered LiMgPdSn-type structure [23]. For the present NiFeMnSn Heusler alloy, the type-I ordered structure is desired to retain a high spin polarization in this system. Such a structure can be achieved with an improved annealing treatment. In the case of Co_2MnGa, it was reported by Kudryavtsev *et al.* [30] that the structural order changed from an amorphous to an $A2$ type and then to a mixed ($A2$ and $B2$) type structure as the annealing temperature was increased up to 753 K. Whereas the sample Co_2MnGa deposited on a substrate at elevated temperature (753 K) exhibited a mixed $B2$- and $L2_1$-type structure with nearly bulk value of magnetization of 3.5 μ_B per formula unit. The quaternary Heusler compounds CoFeMnZ (Z = Al, Ga, Si or Ge) were identified as potential candidates to show half-metallicity by Alijani *et al.* [16] through their *ab initio* electronic structure calculations. However, they also reported site disorder for CoFeMnAl and CoFeMnSi, and expressed the possibility of disorder for CoFeMnGa and CoFeMnGe. In another study, Alijani *et al.* [31] also reported an ∼10% reduction in total measured magnetization per formula unit for NiCoMnGa as compared to its theoretically calculated value. They also stressed the fact that optimization of annealing temperature as well as annealing time is important to obtain a better quality sample with regard to disorder and impurities. In some cases, it was reported that the doping transformed the sample into a half-metallic material. One such example is As and Nb doped quaternary Heusler alloy FeCoZrGe [32]. The study by Nehra *et al.* [33] suggested that the partial substitution of Fe for Co in Co_2CrAl (i.e, CoFeCrAl) eliminated the phase separation which occurred in Co_2CrAl while retaining the half-metallicity and high Curie temperature. However, in the quaternary Heusler alloy NiFeMnSn, studied in the present work, the small difference in the formation energy of the three types (I, II, and III) demands a superior control of the annealing method in achieving the fully ordered type-I LiMgPdSn crystal structure.

IV. SUMMARY

In summary, a high spin polarization at the Fermi level is predicted for the quaternary Heusler alloy NiFeMnSn with the type-I crystal structure from the electronic structure calculation using the full-potential linearized augmented plane-wave (FPLAPW) method within the generalized gradient approximation formalism. A ferromagnetic state is found to be more favorable than the nonmagnetic state with Mn carrying most of the local magnetic moment. The x-ray diffraction study confirms the cubic Heusler structure for the sample prepared using the arc-melting technique. The magnetization measurements indeed indicate the paramagnetic to ferromagnetic phase transition with the Curie temperature well above room temperature. The Mössbauer spectroscopy reveals site disorder for this alloy. The neutron diffraction study quantifies the presence of atomic site disorder along with a ferromagnetic ordering. The electronic structure calculation, performed assuming the atomic site disorder, shows that the site disorder destroys the nearly half-metallic nature of the Heusler alloy NiFeMnSn. Further study on order-disorder crystal structures in quaternary Heusler alloy systems is necessary to correlate their magnetic properties with the theoretically predicted properties. We predict the present compound to show a high degree of spin polarization (76%) at the Fermi level (E_F) for the perfectly LiMgPdSn-type ordered type-I crystal structure indicating the potential usefulness of this system, under the structurally ordered state, in spintronics applications. The present study underlines the importance of achieving fully ordered Heusler alloys by a fine control of the sample preparation for their higher spin polarization.

ACKNOWLEDGMENTS

Syamashree Roy participated in this work during her study leave from School of Physics, University of Hyderabad, Hyderabad 500046, India. M.D.M. acknowledges the useful discussion with A. K. Bera for the analysis of neutron diffraction data.

[1] M. I. Katsnelson, V. Y. Irkhin, L. Chioncel, A. I. Lichtenstein, and R. A. De Groot, Rev. Mod. Phys. **80**, 315 (2008).
[2] R. A. de Groot, F. M. Mueller, P. G. van Engen, and K. H. J. Buschow, Phys. Rev. Lett. **50**, 2024 (1983).
[3] R. A. de Groot, F. M. Mueller, P. G. van Engen, and K. H. J. Buschow, J. Appl. Phys. **55**, 2151 (1984).
[4] C. Felser, G. H. Fecher, and B. Balke, Angew. Chem. Int. Ed. **46**, 668 (2007).
[5] S. A. Wolf, D. D. Awschalom, R. A. Buhrman, J. M. Daughton, S. von Molnár, M. L. Roukes, A. Y. Chtchelkanova, and D. M. Treger, Science **294**, 1488 (2001).
[6] I. Galanakis, P. H. Dederichs, and N. Papanikolaou, Phys. Rev. B **66**, 174429 (2002).
[7] I. Galanakis, P. H. Dederichs, and N. Papanikolaou, Phys. Rev. B **66**, 134428 (2002).
[8] A. N. Vasil'ev, A. D. Bozhko, V. V. Khovailo, I. E. Dikshtein, V. G. Shavrov, V. D. Buchelnikov, M. Matsumoto, S. Suzuki, T. Takagi, and J. Tani, Phys. Rev. B **59**, 1113 (1999).
[9] J. Liu, T. Gottschall, K. Skokov, J. Moore, and O. Gutfleisch, Nat. Mater. **11**, 620 (2012).
[10] R. Suzuki and T. Kyono, J. Alloys Compd. **377**, 38 (2004).
[11] H. A. Kierstead, B. D. Dunlap, S. K. Malik, A. M. Umarji, and G. K. Shenoy, Phys. Rev. B **32**, 135 (1985).
[12] W. Li, J. Cao, J. Ding, and X. Yan, Eur. Phys. J. B **85**, 250 (2012).
[13] I. Galanakis, K. Özdoğan, B. Aktaş, and E. Şaşıoğlu, Appl. Phys. Lett. **89**, 042502 (2006).
[14] L. Bainsla and K. G. Suresh, Appl. Phys. Rev. **3**, 031101 (2016).
[15] H. S. Goripati, T. Furubayashi, Y. K. Takahashi, and K. Hono, J. Appl. Phys. **113**, 043901 (2013).
[16] V. Alijani, S. Ouardi, G. H. Fecher, J. Winterlik, S. S. Naghavi, X. Kozina, G. Stryganyuk, C. Felser, E. Ikenaga, Y. Yamashita *et al.*, Phys. Rev. B **84**, 224416 (2011).
[17] Y. Feng, H. Chen, H. Yuan, Y. Zhou, and X. Chen, J. Magn. Magn. Mater. **378**, 7 (2015).
[18] P. Blaha, K. Schwarz, G. K. H. Madsen, D. Kvasnicka, and J. Luitz, *WIEN2k, An Augmented Plane Wave + Local Orbitals Program for Calculating Crystal Properties* (Karlheinz Schwarz, Techn. Universitaet Wien, Wien, Austria, 2001).
[19] J. P. Perdew, K. Burke, and M. Ernzerhof, Phys. Rev. Lett. **77**, 3865 (1996).
[20] T. Roisnel and J. Rodríguez-Carvajal, Computer code WINPLOTR: a Windows tool for powder diffraction patterns analysis, in *Materials Science Forum, Proceedings of the Seventh European Powder Diffraction Conference (EPDIC 7)*, 2000, pp. 118–123, edited by R. Delhez and E. J. Mittenmeijer; J. Rodríguez-Carvajal and T. Roisnel, Computer code FULLPROF.98 and WINPLOTR: New Windows 95NT Applications for Diffraction Commission For Powder Diffraction, International Union for Crystallography, Newsletter No. 20 (May–August) Summer 1998.
[21] L. Bainsla, K. G. Suresh, A. K. Nigam, M. Manivel Raja, B. S. D. C. S. Varaprasad, Y. K. Takahashi, and K. Hono, J. Appl. Phys. **116**, 203902 (2014).
[22] L. Bainsla, A. I. Mallick, M. M. Raja, A. K. Nigam, B. S. D. C. S. Varaprasad, Y. K. Takahashi, A. Alam, K. G. Suresh, and K. Hono, Phys. Rev. B **91**, 104408 (2015).
[23] M. Halder, M. D. Mukadam, K. G. Suresh, and S. M. Yusuf, J. Magn. Magn. Mater. **377**, 220 (2015).
[24] M. Halder, S. M. Yusuf, A. Kumar, A. K. Nigam, and L. Keller, Phys. Rev. B **84**, 094435 (2011).
[25] J. Kübler, Physica B+C **127**, 257 (1984).
[26] A. D. Svyazhin, E. I. Shreder, V. I. Voronin, I. F. Berger, and S. E. Danilov, J. Exp. Theor. Phys. **116**, 452 (2013).
[27] T. Shinohara, K. Sasaki, H. Yamauchi, H. Watanabe, H. Sekizawa, and T. Okada, J. Phys. Soc. Jpn. **50**, 2904 (1981).
[28] Z. Gercsi, A. Rajanikanth, Y. K. Takahashi, K. Hono, M. Kikuchi, N. Tezuka, and K. Inomata, Appl. Phys. Lett. **89**, 082512 (2006).
[29] Y. Miura, K. Nagao, and M. Shirai, Phys. Rev. B **69**, 144413 (2004).
[30] Y. V. Kudryavtsev, V. A. Oksenenko, Y. P. Lee, Y. H. Hyun, J. B. Kim, J. S. Park, S. Y. Park, and J. Dubowik, Phys. Rev. B **76**, 024430 (2007).
[31] V. Alijani, J. Winterlik, G. H. Fecher, S. S. Naghavi, and C. Felser, Phys. Rev. B **83**, 184428 (2011).
[32] G.-Y. Mao, X.-X. Liu, Q. Gao, L. Li, H.-H. Xie, G. Lei, and J.-B. Deng, J. Magn. Magn. Mater. **398**, 1 (2016).
[33] J. Nehra, V. D. Sudheesh, N. Lakshmi, and K. Venugopalan, Phys. Status Solidi (RRL) **7**, 289 (2013).